

# *Pparg*-P465L Mutation Worsens Hyperglycemia in *Ins2-Akita* Female Mice via Adipose-Specific Insulin Resistance and Storage Dysfunction

Avani A. Pendse,<sup>1</sup> Lance A. Johnson,<sup>1</sup> Yau-Sheng Tsai,<sup>2</sup> and Nobuyo Maeda<sup>1</sup>

**OBJECTIVE**—The dominant-negative P467L mutation in peroxisome proliferator activated receptor- $\gamma$  (PPAR $\gamma$ ) was identified in insulin-resistant patients with hyperglycemia and lipodystrophy. In contrast, mice carrying the corresponding *Pparg*-P465L mutation have normal insulin sensitivity, with mild hyperinsulinemia. We hypothesized that murine *Pparg*-P465L mutation leads to covert insulin resistance, which is masked by hyperinsulinemia and increased pancreatic islet mass, to retain normal plasma glucose.

**RESEARCH DESIGN AND METHODS**—We introduced in *Pparg*<sup>P465L/+</sup> mice an *Ins2-Akita* mutation that causes improper protein folding and islet apoptosis to lower plasma insulin.

**RESULTS**—Unlike *Ins2*<sup>Akita/+</sup> littermates, male *Pparg*<sup>P465L/+</sup> *Ins2*<sup>Akita/+</sup> mice have drastically reduced life span with enhanced type 1 diabetes. Hyperglycemia in *Ins2*<sup>Akita/+</sup> females is mild. However, *Pparg*<sup>P465L/+</sup> *Ins2*<sup>Akita/+</sup> females have aggravated hyperglycemia, smaller islets, and reduced plasma insulin. In an insulin tolerance test, they showed smaller reduction in plasma glucose, indicating impaired insulin sensitivity. Although gluconeogenesis is enhanced in *Pparg*<sup>P465L/+</sup> *Ins2*<sup>Akita/+</sup> mice compared with *Ins2*<sup>Akita/+</sup>, exogenous insulin equally suppressed gluconeogenesis in hepatocytes, suggesting that *Pparg*<sup>P465L/+</sup> *Ins2*<sup>Akita/+</sup> livers are insulin sensitive. Expression of genes regulating insulin sensitivity and glycogen and triglyceride contents suggest that skeletal muscles are equally insulin sensitive. In contrast, adipose tissue and isolated adipocytes from *Pparg*<sup>P465L/+</sup> *Ins2*<sup>Akita/+</sup> mice have impaired glucose uptake in response to exogenous insulin. *Pparg*<sup>P465L/+</sup> *Ins2*<sup>Akita/+</sup> mice have smaller fat depots composed of larger adipocytes, suggesting impaired lipid storage with subsequent hepatomegaly and hypertriglyceridemia.

**CONCLUSIONS**—PPARG-P465L mutation worsens hyperglycemia in *Ins2*<sup>Akita/+</sup> mice primarily because of adipose-specific insulin resistance and altered storage function. This underscores the important interplay between insulin and PPAR $\gamma$  in adipose tissues in diabetes. *Diabetes* 59:2890–2897, 2010

From the <sup>1</sup>Department of Pathology and Laboratory Medicine, The University of North Carolina at Chapel Hill, Chapel Hill, North Carolina; and the <sup>2</sup>Institute of Clinical Medicine, College of Medicine, National Cheng Kung University, Tainan, Taiwan, Republic of China.

Corresponding author: Nobuyo Maeda, nobuyo@med.unc.edu.

Received 11 May 2010 and accepted 6 August 2010. Published ahead of print at <http://diabetes.diabetesjournals.org> on 19 August, 2010. DOI: 10.2337/db10-0673.

© 2010 by the American Diabetes Association. Readers may use this article as long as the work is properly cited, the use is educational and not for profit, and the work is not altered. See <http://creativecommons.org/licenses/by-nc-nd/3.0/> for details.

The costs of publication of this article were defrayed in part by the payment of page charges. This article must therefore be hereby marked "advertisement" in accordance with 18 U.S.C. Section 1734 solely to indicate this fact.

**D**iabetes is a major health care challenge in itself and significantly increases cardiovascular disease morbidity and mortality. As a multifactorial, chronic disease, diabetes emanates from the complex interaction of genetic and environmental influences. Among the many factors presumed or shown to contribute to its pathology, peroxisome proliferator activated receptor- $\gamma$  (PPAR $\gamma$ ) is an important candidate. PPAR $\gamma$  is a nuclear receptor and is necessary for adipocyte differentiation and triglyceride deposition (1). Activation of PPAR $\gamma$  has already provided therapeutic potential. One group of its synthetic ligands, the thiazolidinedione drugs, has found applications as antidiabetic agents (2).

Various point mutations in PPAR $\gamma$  that affect adipose tissue distribution and insulin sensitivity have been identified in humans. For example, the PPARG-P12A polymorphism in humans is associated with reduced body weight and increased insulin sensitivity (3). Increased PPAR $\gamma$  activity in PPARG-P115Q mutation is associated with severe obesity and mild insulin resistance (4). Conversely, two dominant negative mutations resulting in decreased PPAR $\gamma$  activity, PPARG-P467L and PPARG-V290M, were reported in patients with severe insulin resistance (5). To date, different mouse models have demonstrated the role of PPAR $\gamma$  in varied metabolic processes. Lack of *Pparg* causes embryonic lethality in mice (6,7), and the *Pparg*-null embryos have no perceptible adipose tissue (6,8). Tissue-specific *Pparg* knockouts in liver (9) and skeletal muscle (10) exhibit insulin resistance. In contrast, absence of *Pparg* in  $\beta$ -cells does not affect glucose homeostasis, although it increases  $\beta$ -cell mass (11). Animals entirely lacking *Pparg* are nonviable, and tissue-specific knockouts offer a strategy for artificial manipulation that is only possible within experimental settings. Thus, an important step is to extend this work to study the role of PPAR $\gamma$  in a context applicable to human patients.

The dominant-negative heterozygous PPARG-P467L mutation was originally identified in patients with severe insulin resistance, hyperglycemia, lipodystrophy, and hypertension (5). However, mice carrying the corresponding *Pparg*-P465L mutation (L/+ or L) exhibit normal plasma glucose and insulin sensitivity (12,13). These mice have mild hyperinsulinemia and increased pancreatic islet mass, especially on high-fat diet (12). In this study, we attempted to understand whether the observed insulin-resistance phenotype in human patients is indeed attributable to L/+ mutation or a mere association. We hypothesized that mice carrying the L/+ mutation have covert insulin resistance; however, the simultaneous occurrence of islet hyperplasia and hyperinsulinemia com-

pensates for this insulin resistance to retain normal plasma glucose.

Improper folding of insulin due to the C96Y *Ins2-Akita* mutation causes endoplasmic reticulum stress and  $\beta$ -cell apoptosis, leading to reduced plasma insulin (14). The mutation only affects  $\beta$ -cells, and the heterozygous Akita mice develop consistently elevated plasma glucose levels early in postnatal life. Consequently, Akita model is uniquely suited to test our prediction that, with reduced insulin production, the *Pparg*<sup>P465L/+</sup> mice would be unable to compensate for the peripheral insulin resistance. We show here that the Akita females with *Pparg*<sup>P465L/+</sup> mutation have increased severity of hyperglycemia and insulin resistance restricted to adipose tissue.

## RESEARCH DESIGN AND METHODS

***Pparg*<sup>P465L/+</sup> *Ins2*<sup>Akita/+</sup> double mutant mice.** Heterozygous male *Pparg*<sup>P465L/+</sup> mice on 129/SvEvTac background (12) were mated with heterozygous female *Ins2*<sup>Akita/+</sup> mice on C57BL/6J background (Jackson Lab stock no. 003548). Experimental mice were F1 littermates: *Pparg*<sup>P465L/+</sup> *Ins2*<sup>Akita/+</sup> (LA), *Pparg*<sup>+/+</sup> *Ins2*<sup>Akita/+</sup> (WA), *Pparg*<sup>P465L/+</sup> *Ins2*<sup>+/+</sup> (L+), and wild-type (W+) used at 3 and 7 months for characterization of hyperglycemia and to define the organ-specific phenotype, respectively. Mice were fed regular chow (LabDiet 5P76; PMI Nutrition International) and were handled with Institutional Animal Care and Use Committees approved procedures.

**Biochemical determinations.** Plasma concentrations of glucose, cholesterol, nonesterified free fatty acids (NEFAs), and 3-hydroxybutyrate (3-HB) were determined by kits from Wako (Richmond, VA). Triglyceride concentrations were determined using kits from Stanbio (San Antonio, TX). Plasma insulin and leptin were determined by ELISA (Crystal Chem Inc., Chicago, IL). Pooled plasma samples (100  $\mu$ l) were fractionated by fast protein liquid chromatography using Superose 6 HR10/30 column (GE Healthcare, Piscataway, NJ). Plasma adiponectin was measured by an ELISA using murine adiponectin-specific antibody (Sigma, St Louis, MO). Tissue glycogen content was determined as difference of glucose contents before and after digestion with *Aspergillus niger* amyloglycosidase (Sigma no. 046K8801) as described (15).

**Oral glucose tolerance test.** After 4-h fast, 7-month-old female mice were administered 1.3 mg/g body weight of D-glucose (Columbus Chemical Industries Inc, Columbus, WI) by oral gavage. Blood was collected before and at indicated times after glucose administration to determine plasma glucose.

**Intraperitoneal insulin tolerance test.** An intraperitoneal insulin tolerance test (IPITT) was performed. After 4-h fast, 7-month-old female mice were injected intraperitoneally with insulin (Novolin; 0.5 units/kg body weight; Novo Nordisk Inc, Princeton, NJ). Blood was collected before and at indicated times after insulin injections to determine plasma glucose and NEFA.

**Insulin-stimulated glucose uptake in adipose tissue.** Inguinal and gonadal adipose tissues from two female mice from each genotype were cut into small pieces (20–40 mg) under aseptic conditions and incubated in high glucose Dulbecco's modified Eagle's medium supplemented with 100 IU/ml penicillin and 100  $\mu$ g/ml streptomycin (Sigma-Aldrich, St Louis, MO) in the absence or presence of 100 nmol/l insulin (insulin solution from bovine pancreas; Sigma-Aldrich). After 24 h, glucose reduction in the medium was measured and results were normalized to explant weight (16,17).

**Gene expression.** Total RNA was purified using Automated Nucleic Acid Workstation ABI 6,700, and real-time PCR was performed in ABI PRISM 7,700 Sequence Detector (Applied Biosystems).  $\beta$ -actin mRNA was used for normalization. Primers and probes are available on request.

**Morphological analysis.** Paraffin sections from adipose tissue and pancreas of female mice ( $n \geq 4$ ) were stained with hematoxylin–eosin. Adipocyte size was measured in  $\sim 250$  cells per mouse using ImageJ software. Mean pancreatic islet area, the average from all islets identified on each section, was determined.

**Pyruvate tolerance test.** After 14-h fast, 3-month-old female mice were injected intraperitoneally with 2 mg/kg body weight of sodium pyruvate (Sigma, St. Louis, MO). Blood was collected before and at indicated times after injection to determine plasma glucose.

**Glucose production from primary hepatocytes.** Primary hepatocytes were isolated as described (18) and plated on mouse-collagen IV coated plates. Cells were washed twice with PBS to remove glucose and incubated for 16 h in 500  $\mu$ l medium containing 10 nmol/l dexamethasone, 0.5 mmol/l isobutylmethylxanthine with and without 2 mmol/l sodium pyruvate, and 100 nmol/l insulin. Glucose concentration was measured in 100  $\mu$ l medium.

**2-deoxyglucose uptake.** Hepatocytes were plated at 100,000 cells per well in a 24-well plate and maintained in hepatocyte culture medium (Xenotech, Lenexa, KS) for 24 h. The cells were washed with PBS and maintained in serum-free medium containing 135 mmol/l NaCl, 5.4 mmol/l KCl, 1.4 mmol/l CaCl<sub>2</sub>, 1.4 mmol/l MgSO<sub>4</sub>, and 10 mM Na<sub>4</sub>P<sub>2</sub>O<sub>7</sub> for 30 min (19). 2-Deoxy-D-[1-<sup>3</sup>H]glucose (Perkin-Elmer) was added to a final concentration of 1  $\mu$ Ci/ml, and cells were incubated for 10 min (20). Cells were washed three times with PBS and solubilized in 1 ml 1% SDS. Radioactivity in 350  $\mu$ l aliquots was measured in a scintillation counter. Glucose uptake was normalized to protein content and expressed as milligrams of glucose per gram of protein. In a similar experiment, primary adipocytes were isolated and 2-deoxy-D-[1-<sup>3</sup>H]glucose (Perkin-Elmer) uptake was measured in the absence or presence of 100 nmol/l insulin as previously described (21,22).

**Data analysis.** Values are reported as mean  $\pm$  SEM. Statistical analyses were conducted using two-way ANOVA with *Pparg* and *Ins2* genotypes as two factors. Student *t* test was used for comparisons between groups, and differences were considered to be statistically significant if  $P < 0.05$ .

## RESULTS

**Increased hyperglycemia in *Ins2*<sup>Akita/+</sup> mice carrying the *Pparg*-P465L mutation.** From our breeding scheme, we obtained F1 mice with four genotypes: wild-type (W+), *Pparg*<sup>P465L/+</sup> (L+), *Ins2*<sup>Akita/+</sup> (WA), and *Pparg*<sup>P465L/+</sup> *Ins2*<sup>Akita/+</sup> (LA) mice. The mice were born in the expected Mendelian ratio; however, all LA male mice died before 150 days, demonstrating significantly reduced survival (Fig. 1A). In contrast, >85% WA males survived and all W+ and L+ males survived to this age. Younger LA males at 6 weeks of age had higher fasting plasma glucose (LA, 577  $\pm$  31, and WA, 494  $\pm$  40 mg/dl,  $n = 6$ ; Fig. 1B) and triglyceride compared with WA mice, although these increases did not reach significance (supplementary Fig. 1A, available in an online appendix at <http://diabetes.diabetesjournals.org/cgi/content/full/db10-0673/DC1>). However, LA males had significantly higher fasting plasma ketone body levels (LA, 407  $\pm$  23, and WA, 271  $\pm$  40  $\mu$ mol/l,  $n \geq 4$ ;  $P < 0.05$ , Fig. 1C), indicating a severe lack of insulin and/or insulin resistance.

In contrast to LA males, LA females demonstrated normal survival throughout 7 months of the study period. We therefore focused on WA and LA females to understand the effects of *Pparg*-P465L mutation on peripheral insulin sensitivity and diabetes severity. Basic characterization of a set of 3-month-old mice is shown in supplementary Table 1, available in an online appendix. The LA double-mutant females had significantly higher fasting plasma glucose compared with WA littermate controls. This increase in plasma glucose was apparent at 3 months of age (LA, 508  $\pm$  23,  $n = 6$  vs. WA, 354  $\pm$  36 mg/dl,  $n = 13$ ;  $P < 0.01$ ) and was maintained throughout the study period of  $\sim 7$  months (LA, 369  $\pm$  38,  $n = 6$  vs. WA, 273  $\pm$  24 mg/dl,  $n = 13$ ;  $P < 0.05$ , Fig. 1D). The LA females had significantly high fasting plasma triglyceride levels at both 3 months and 7 months of age (LA, 78  $\pm$  12 and 65  $\pm$  6, WA, 51  $\pm$  3 and 45  $\pm$  3 mg/dl,  $n = 6$ ;  $P < 0.01$ , Fig. 1E). As expected in a diabetic state, this increase in plasma triglyceride level was mainly due to increase in the VLDLs (supplementary Fig. 1B). Diabetes, with its low levels of functional insulin, is the most common pathological cause of elevated ketone bodies (23). Consistently, LA females had significantly higher levels of 3-hydroxybutyrate compared with WA mice after 4 h of fasting (LA, 395  $\pm$  63,  $n = 8$ , and WA, 222  $\pm$  37  $\mu$ mol/l,  $n = 7$ ;  $P < 0.05$ , Fig. 1F).

We next performed an oral glucose tolerance test, where LA females had significantly higher plasma glucose levels at various time points up to 2 h after administration of glucose load (Fig. 2A). Fifteen min after glucose challenge, the LA female mice had significantly lower plasma

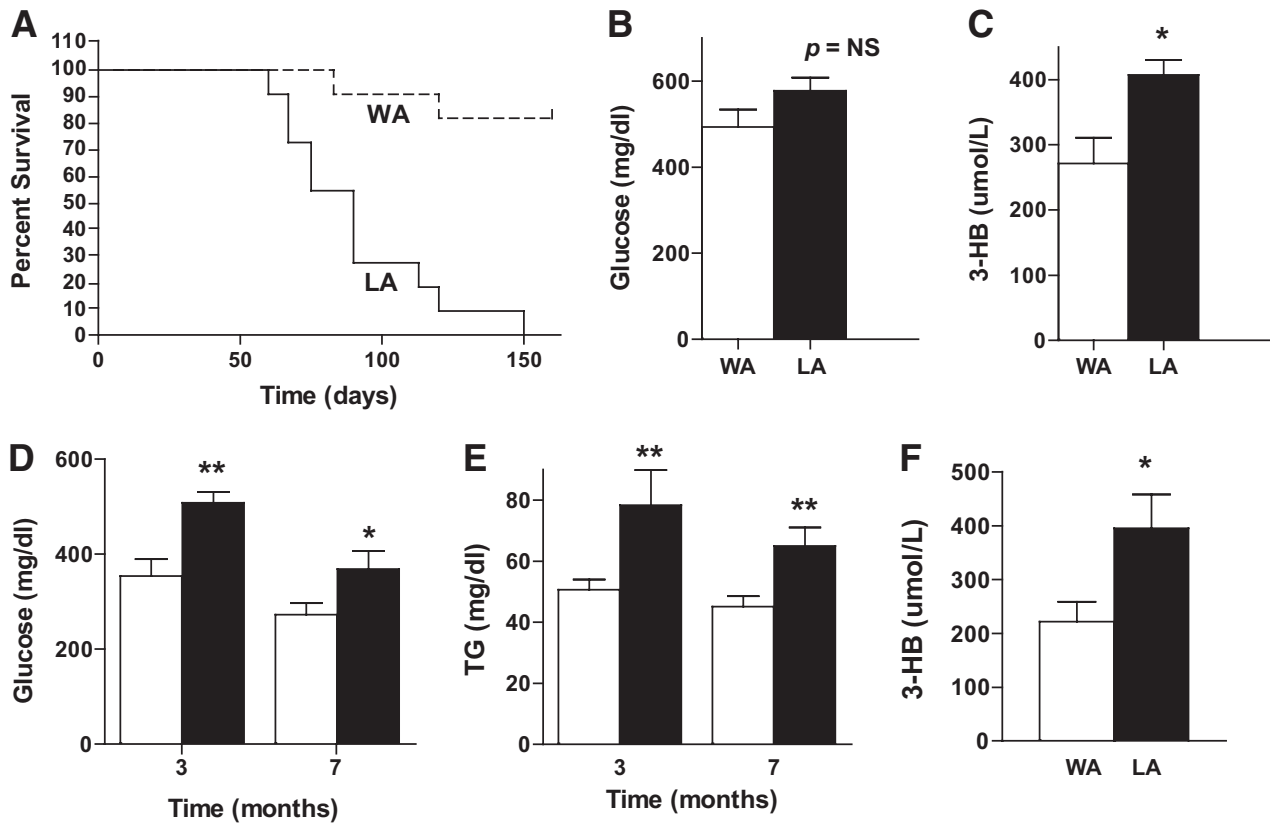


**FIG. 1.** Increased hyperglycemia in *Ins2*<sup>Akita/+</sup> mice carrying the *PPAR* $\gamma$ <sup>P465L/+</sup> mutation. **A:** Reduced survival in male LA ( $n = 12$ , solid line) mice compared with WA ( $n = 12$ , dashed line) littermates. **B:** Fasting plasma glucose in 6-week-old male LA mice ( $n = 10$ , black bars) compared with male WA littermates ( $n = 12$ , white bars). **C:** Fasting plasma ketone body (3-hydroxybutyrate) levels in 6-week-old male LA mice ( $n = 4$ ) compared with male WA littermates ( $n = 6$ ). **D and E:** Fasting plasma glucose and triglyceride levels in female LA (black bars) and WA (white bars) littermates at 3 and 7 months of age ( $n \geq 6$ ). **F:** Fasting plasma ketone bodies in 3-month-old female LA ( $n = 6$ ) and WA ( $n = 7$ ) littermates. \* $P < 0.05$ , \*\* $P < 0.01$ . 3-HB, 3-hydroxybutyrate; NS, not significant; TG, triglyceride.

insulin levels compared with WA mice (LA,  $0.36 \pm 0.01$ ,  $n = 4$ , and WA,  $0.49 \pm 0.03$  ng/ml,  $n = 6$ ;  $P = 0.01$ , Fig. 2B). This lower glucose-stimulated insulin level in LA mice was accompanied by significantly smaller mean pancreatic islet area when compared with age-matched WA controls (Fig. 2C and supplementary Fig. 1C and D). Thus, the *Pparg*-P465L mutation worsens the hyperglycemia caused by *Ins2*-Akita mutation partly by inadequate secretion of glucose-stimulated insulin.

**Adipose tissue dysfunction contributes to insulin resistance in the LA females.** We next investigated whether insulin resistance contributes to higher plasma glucose levels in female LA mice, using an IPITT. Insulin-mediated suppression of plasma glucose was impaired in LA females. Plasma glucose in WA females dropped to  $70 \pm 6\%$  compared with baseline at 15 min after an intraperitoneal insulin injection. However, in LA females, the glucose levels reduced only to  $94 \pm 4\%$  ( $n = 6$ ,  $P <$

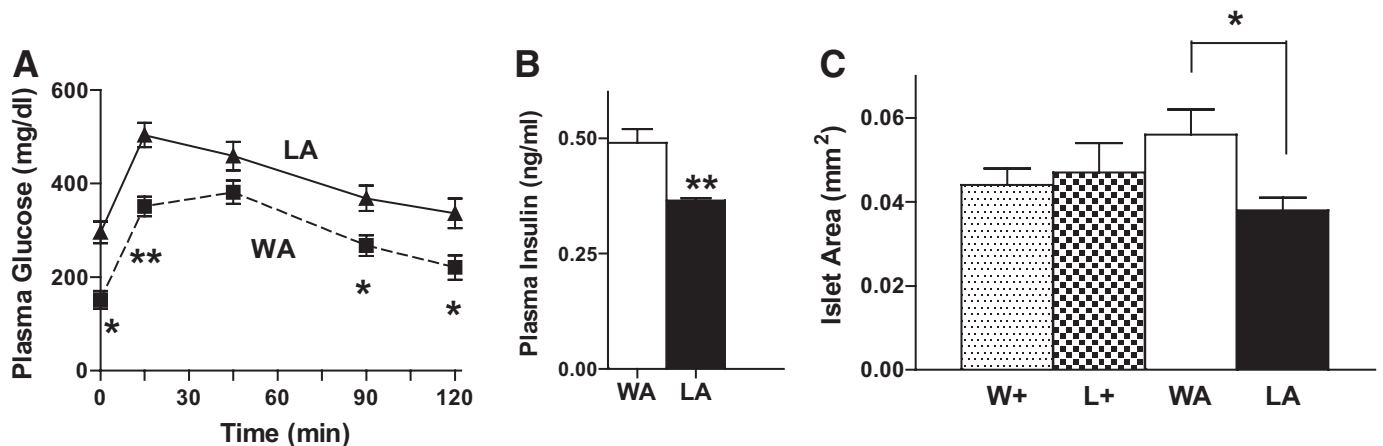


**FIG. 2.** Reduced circulating insulin contributes to hyperglycemia in female LA mice. **A:** Plasma glucose levels after oral glucose load and **(B)** plasma insulin levels at 15 min after oral glucose administration in female LA mice ( $n = 5$ ) compared with female WA littermates ( $n = 5$ ). **C:** Mean pancreatic islet area in female W+ ( $n = 4$ ), L+ ( $n = 4$ ), LA mice ( $n = 5$ ), and WA littermates ( $n = 6$ ). \* $P < 0.05$ , \*\* $P < 0.01$ . Dashed line and white bars indicate WA; solid line and black bars indicate LA; W+ are speckled bars, and L+ are checkered bars.

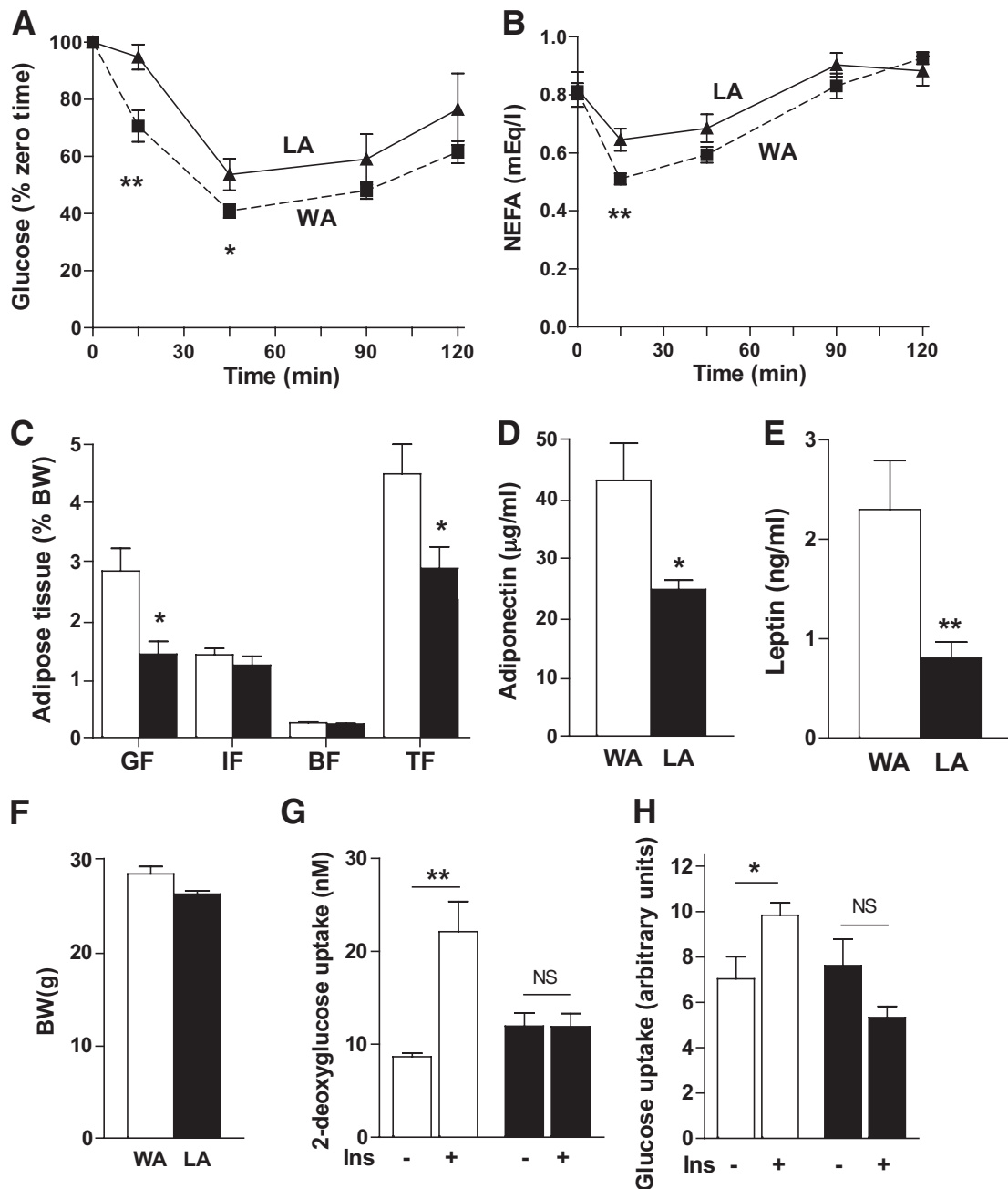


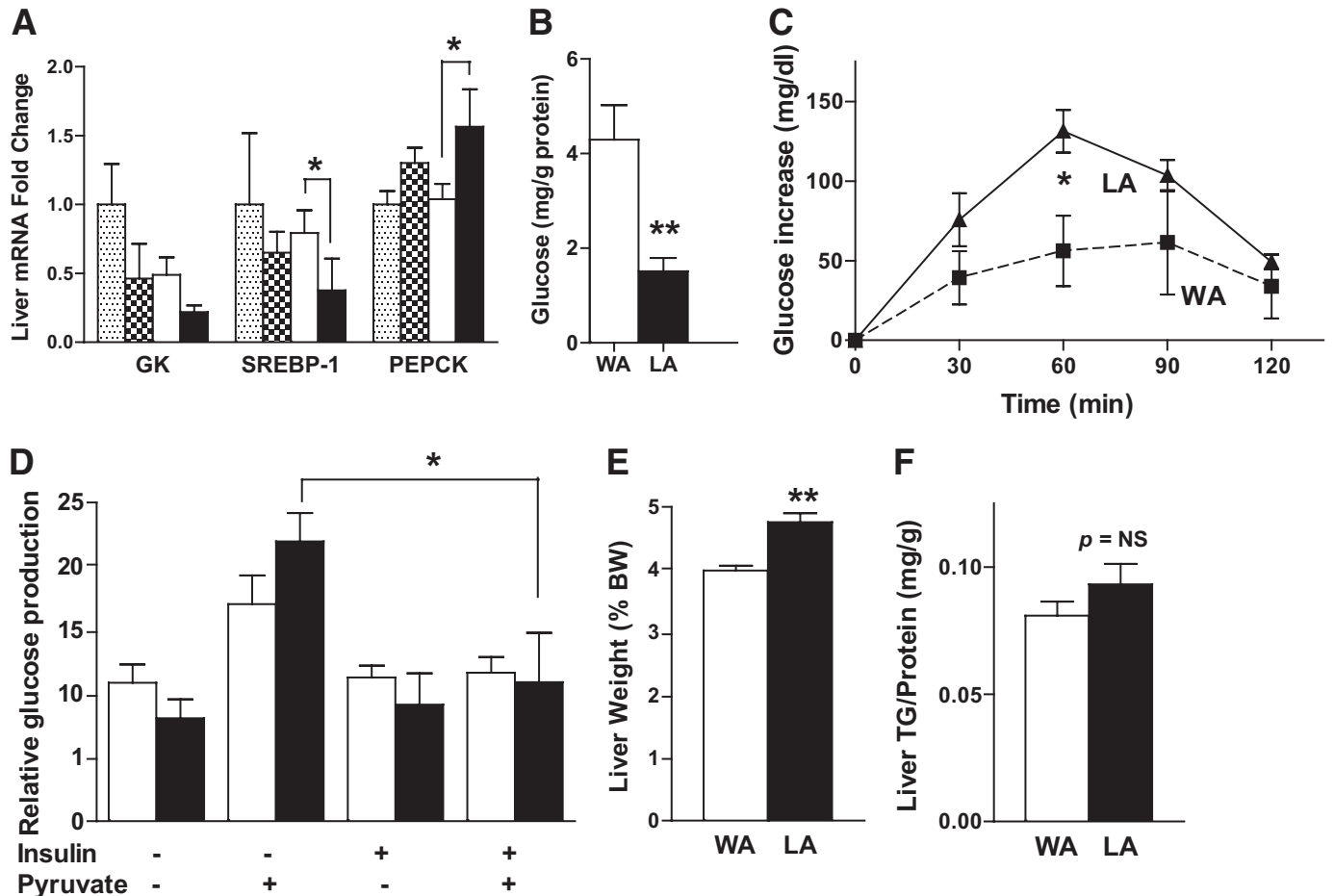
**FIG. 3.** Insulin resistance in adipose tissue of LA female mice. **A:** Blunted fall in plasma glucose and **(B)** suppression of NEFA secretion in LA mice ( $n = 5$ , solid line) compared with WA littermates ( $n = 6$ , dotted line) in response to intraperitoneally administered insulin 0.5 U/kg body weight. **C:** Adipose tissue weight normalized with body weight of 3-month-old female LA ( $n = 7$ , black bars) and WA mice ( $n = 7$ , white bars). GF, perigonadal fat; IF, inguinal fat; BF, brown fat, and TF, total fat. **D:** Plasma adiponectin and **(E)** leptin and **(F)** body weight in LA ( $n = 6$ ) and WA mice ( $n = 7$ ). Glucose uptake in primary adipocytes **(G)** and adipose tissue explants **(H)**, respectively, without and with 100 nmol/l insulin. \* $P < 0.05$ , \*\* $P < 0.01$ . NS, not significant.

0.01, Fig. 3A). In addition to glucose homeostasis, insulin also suppresses NEFA release, largely from the adipose tissue (24). NEFA levels in LA mice were significantly higher than in WA controls 15 min after insulin injection (LA,  $0.65 \pm 0.04$ ,  $n = 5$ , and WA,  $0.51 \pm 0.02$  mEq/l,  $n = 6$ ;  $P < 0.01$ , Fig. 3B). This suggests that LA mice were not able to suppress the NEFA release as effectively as the WA controls.

PPAR $\gamma$  is widely recognized as an important regulator of adipose tissue differentiation. Mice carrying the *Pparg-P465L* mutation have normal total adipose tissue mass with altered fat distribution (12). Insulin is also known to be an important player in adipose tissue

physiology. LA mice carrying mutations in both these important genes have a significant reduction in their total adipose tissue mass and have lower body weight (Fig. 3C, F). They have reduced gonadal (visceral) adipose tissue (similar to L+ mice) but a slight reduction in inguinal (subcutaneous) adipose tissue (unlike L+ mice, which have a significantly higher inguinal fat mass than W+ mice) (supplementary Table 1). Thus, simultaneous presence of *Pparg-P465L* and *Ins2-Akita* mutations severely compromises the normal adipose tissue development. Median size of individual adipocytes from the inguinal depot was significantly larger in the LA mice than those in the WA mice (supplementary





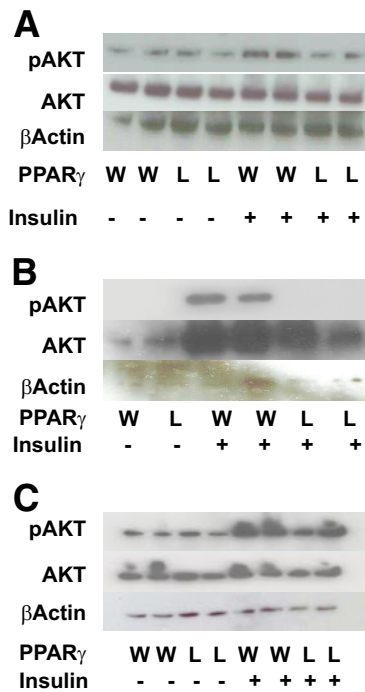
**FIG. 4.** Altered liver function due to reduced plasma insulin levels contributes to increased hyperglycemia in LA mice. **A:** Average mRNA amounts of genes for GK, SREBP-1, and PEPCK in L+ (checked), WA (white), and LA (black) mice relative to that in W+ mice (speckled) as 1.0 ( $n \geq 7$ ). **B:** Uptake of 2-deoxyglucose in primary hepatocytes. **C:** Increase in plasma glucose after an intraperitoneal administration of 2 mg/kg body weight pyruvate in LA female mice compared with WA littermates ( $n = 4$  each). **D:** Glucose production (mg/g protein) in cultured WA (white bars) and LA (black bars) hepatocytes. Increase in glucose in the medium by the addition of 2 mmol/l sodium pyruvate was suppressed by the presence of 100 nmol/l insulin. **E:** Increased liver weight and **(F)** a small increase in liver triglyceride levels in LA mice ( $n = 6$ ) compared with WA mice ( $n = 12$ ). \* $P < 0.05$ , \*\* $P < 0.01$ . NS, not significant.

Fig. 2A, available in an online appendix), and an assessment of gonadal adipocytes suggested a similar change. Together, these data suggest that the adipose tissue in LA mice is composed of fewer, slightly larger adipocytes.

The LA mice also had significantly reduced plasma levels of adiponectin (LA,  $24.4 \pm 1.5$ ,  $n = 3$  vs. WA,  $42.5 \pm 6.2$   $\mu\text{g/ml}$ ,  $n = 3$ ;  $P < 0.05$ , Fig. 3D) and leptin (LA,  $0.8 \pm 0.1$ ,  $n = 8$  vs. WA,  $2.3 \pm 0.5$  ng/ml,  $n = 8$ ;  $P < 0.05$ , Fig. 3E). Adiponectin and leptin are primarily produced in adipose tissue and are critical to maintain insulin sensitivity (25,26). To understand whether reduced amount of adipose tissue and impaired adipokine production extend to impairment in insulin sensitivity, we studied primary adipocytes and adipose tissue explants in vitro. When mature adipocytes were isolated and treated with 100 nmol/l insulin, LA adipocytes had much reduced insulin-stimulated 2-deoxyglucose uptake compared with WA adipocytes (LA,  $11.92 \pm 1.4$  nmol/l vs. WA,  $22.11 \pm 3.23$ ;  $P < 0.05$ , Fig. 3G). Similarly, glucose uptake in adipose tissue explants from WA mice significantly increased upon insulin stimulation. However, glucose uptake in LA explants did not respond to insulin (LA,  $5.3 \pm 0.5$  vs. WA,  $9.8 \pm 0.6$  arbitrary units;  $P = 0.0001$ , Fig. 3H). These data demonstrate the insulin resistance phenotype in the LA adipose

tissue. In separate experiments, both W+ and L+ adipose tissue explants had comparable increases in insulin-stimulated glucose uptake, confirming their normal insulin sensitivity (data not shown). Incubation with insulin induced a twofold increase in phosphorylation of Akt in primary adipocytes from inguinal and gonadal fat of WA mice. In contrast, insulin-stimulated phosphorylation of Akt was significantly blunted in both inguinal and gonadal adipocytes and was not different from the unstimulated cells from LA mice (Fig. 5A and B). The total amount of Akt protein was comparable in the two genotypes. Thus, LA female mice have smaller and less functional adipose tissue, which contributes to the mild insulin-resistance phenotype as observed by IPITT in these mice.

**Increased gluconeogenesis contributes to fasting hyperglycemia in LA mice.** LA livers revealed a 2.2-fold reduced expression of glucokinase, a key glucose uptake enzyme, compared with WA mice ( $P = 0.06$ , Fig. 4A). Analysis with two-way ANOVA suggests that effects of both *Pparg* genotype ( $P < 0.05$ ) and *Ins2* genotype ( $P < 0.05$ ) are significant and additively contributing to the reduced glucokinase expression in LA mice. We observed a twofold reduction in the gene expression of sterol regulatory element binding protein (*SREBP-1*), which binds to and increases the transcription of glucokinase



**FIG. 5.** Insulin-induced Akt phosphorylation. Western blot for pAKT (upper panels), total AKT (middle panels), and  $\beta$ -actin (lower panels) in adipocytes isolated from inguinal fat (A), gonadal fat (B), and hepatocytes (C). Cells were incubated with 100 nmol/l (+) or without (-) insulin for 10 min. Antibodies used were phospho-Akt (Thr308) (Cell Signaling no. 2,965), Akt (Cell Signaling no. 9,272), and  $\beta$ -actin (Cell Signaling no. 5,125). (A high-quality color representation of this figure is available in the online issue.)

gene ( $P < 0.05$ ). However, there was a significant 1.5-fold increase in the gene expression for phosphoenolpyruvate carboxykinase (*PEPCK*) ( $P < 0.05$ ), one of the important regulators of gluconeogenesis. Consistent with the gene expression profile, the uptake of 2-deoxyglucose was significantly lower in primary hepatocytes isolated from LA compared with WA females (WA,  $4.29 \pm 0.7$ , and LA,  $1.51 \pm 0.28$  mg/g protein;  $P < 0.01$ , Fig. 4B).

We next performed a pyruvate tolerance test to assess the rate of gluconeogenesis in WA and LA female mice. LA mice indeed demonstrated a 2.3-fold greater increase in plasma glucose levels compared with WA mice at 60 min after an intraperitoneal injection of pyruvate ( $P < 0.05$ , Fig. 4C). Thus, impairment in glucose uptake with increased hepatic glucose production contributes to the fasting hyperglycemia in LA females compared with WA controls. Corroborating with the in vivo data, glucose

production from primary hepatocytes, isolated from LA mice, increased significantly in the presence of pyruvate (2.7-fold) compared with 1.3-fold in WA hepatocytes. This increase was completely suppressed in the presence of exogenous insulin in both genotypes (Fig. 4D). Furthermore, the Akt phosphorylation in hepatocytes from both WA and LA mice was increased comparably after incubation with 100 nmol/l insulin for 10 min (Fig. 5C). Thus, hepatocytes from LA mice are as sensitive to insulin as those from WA cells. At 7 months of age, the LA female mice also had a small yet significant increase in their liver weight (LA  $4.68 \pm 0.14$ ,  $n = 6$ , and WA  $3.9 \pm 0.08\%$ ,  $n = 12$ ;  $P < 0.05$ , Fig. 4E). This increase is partially explained by a small increase in liver triglyceride content per gram of protein (Fig. 4F). Because the liver weight and triglyceride accumulation were not different in LA and WA female mice at 3 months (supplementary Table 1), the increase in liver weight appears to be an age-dependant phenomenon.

***Pparg*P465L mutation does not affect glucose handling and insulin sensitivity in the skeletal muscle.** The mRNA level of *Glut-4*, the major insulin-sensitive glucose transporter in skeletal muscle, showed no change in LA mice compared with WA mice. Expression levels of *AdipoR1*, *IR*, and *IRS-1*, genes important for normal insulin sensitivity, were also unchanged (Fig. 6A and supplementary Tables 2 and 3, available in an online appendix). Insulin resistance is usually associated with increased intracellular accumulation of lipids (27); however, the skeletal muscle triglyceride levels were unaltered by the presence of *Pparg*-P465L mutation (Fig. 6B). Glycogen content was increased in mice with the *Akita* mutation, but *Pparg*-P465L mutation had no effects (Fig. 6C). Taken together, these data indicate that glucose handling and insulin sensitivity in skeletal muscle are largely unaffected by *Pparg*-P465L mutation.

## DISCUSSION

Glucose tolerance and insulin resistance are complex phenomena affected by multiple signaling mechanisms in varied organs. For an individual as a whole, the implications of being hyperglycemic and insulin resistant are serious. In this study, we focused on a dominant negative point mutation, *Pparg*-P465L, in the ligand-binding domain of PPAR $\gamma$  and established that this mutation can worsen the hyperglycemia caused by the diabetogenic *Ins2-Akita* mutation. The higher plasma glucose in female LA mice compared with WA females can be accounted for by adipose tissue-specific insulin resistance, reduced circulating plasma insulin, and increased gluconeogenesis.

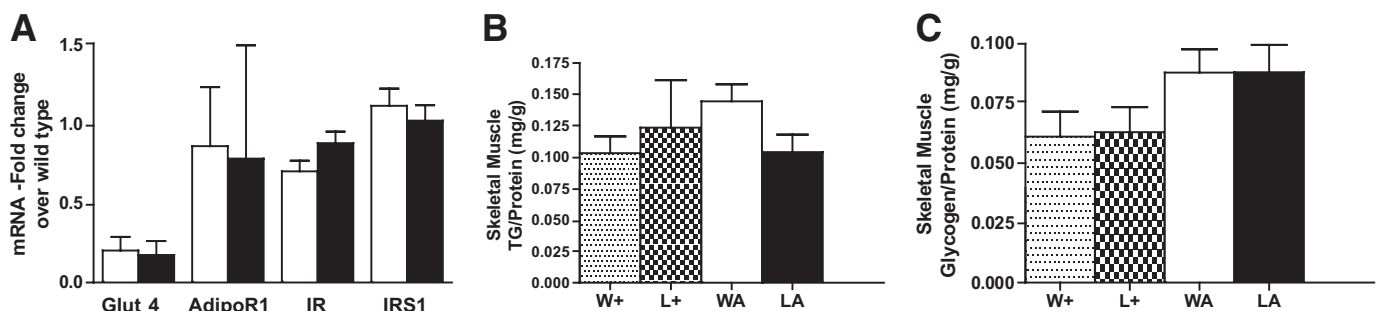


**FIG. 6.** Normal glucose handling in skeletal muscle. A: Gene expression of *Glut4*, *AdipoR1*, *IR*, and *IRS-1* in female WA (white bars) and LA (black bars) mice. Data are expressed as mean  $\pm$  SE relative to the mean level in wild-type animals set as 1.0. B: Triglyceride content per gram of protein in skeletal muscle in female mice. C: Skeletal muscle glycogen storage per gram of protein in female mice.

*Pparg* is expressed in pancreatic islets, where it has a growth inhibitory role. Targeted elimination of *Pparg* in  $\beta$ -cells led to bigger pancreatic islet mass without alterations in glucose homeostasis (11). Unlike the wild-type islets, *Pparg*-deficient islets lack the ability to expand in response to high-fat diet (11). In contrast, mice carrying the *Pparg*-P465L mutation also have bigger islets, particularly on a high-fat diet (12). Therefore, although the *Pparg*-P465L mutation is unable to exert a normal growth inhibitory action, it does not interfere with the expansion of islets in response to high-fat feeding. In our current study of mice with *Ins2*-Akita mutation, the LA females had significantly smaller mean islet area compared with the WA islets, which are enlarged. The LA females also had reduced plasma insulin levels 15 min after an oral glucose dose compared with the WA littermates. Although the direct effect of the *Pparg*-P465L mutation cannot be excluded, it is likely that the increased insulin demand from the already stressed pancreas accelerates apoptosis of  $\beta$ -cells initiated by the *Ins2*-Akita mutation and contributes to the augmented hyperglycemia seen in LA mice. Consistent with our observation, Evans-Mollina et al. in 2009 demonstrated the positive effects of PPAR $\gamma$  agonist Pioglitazone on islet function in diabetic mice as measured by higher random insulin levels and improved glucose-stimulated insulin release (28). These improvements were secondary to reduced endoplasmic reticulum stress and improved expression profile of genes involved in glucose sensing and  $\beta$ -cell differentiation.

Our studies have shown that LA mice have increased fasting plasma glucose levels and an insulin-resistance phenotype. In fasted states, liver is the main source of plasma glucose where pyruvate, amino acids, and glycerol are converted into glucose through gluconeogenesis. This newly synthesized glucose is available as energy for tissues, in particular the brain, which relies primarily on carbohydrate metabolism (29). Twofold reductions in hepatic *GK* expression in LA mice result in reduced glucose uptake. The glucokinase promoter has a peroxisome proliferator response element and is transcriptionally activated by PPAR $\gamma$  agonists (30). Hepatic *GK* expression is reduced in diabetic animal models with insulin deficiency (31), and insulin has been shown to be a major activator of *GK* gene transcription (31,32) through the transcription factor *SREBP-1c* (30). We in turn observed a significant decrease in *SREBP-1c* expression in LA compared with WA livers. Thus, reduced circulating insulin levels and *Pparg*-P465L mutation have an additive effect to reduce *GK* expression. In addition, the upregulation of *PEPCK* in these mice suggests increased gluconeogenesis, which could explain the higher fasting plasma glucose in LA mice. A pyruvate tolerance test, where LA mice showed a significantly larger increase in glucose after pyruvate injection, as well as higher pyruvate-stimulated glucose production in the isolated LA hepatocytes than WA hepatocytes in culture, confirmed this possibility. Thus, the reduced hepatocyte glucose uptake coupled with upregulated gluconeogenesis contributes to higher plasma glucose in LA compared with WA females. Increased hepatic gluconeogenesis in LA females could possibly result from a deficiency in circulating insulin and/or insulin resistance. Our experiments showing that LA hepatocytes are able to suppress glucose production from pyruvate in response to exogenous insulin suggest that the increased hepatic gluconeogenesis observed in LA mice mainly results from a

deficiency in circulating insulin but not hepatic insulin resistance.

The insulin-resistance phenotype observed in the LA females primarily arises from the adipose tissue. PPAR $\gamma$  and insulin are both widely recognized as essential genes for adipose tissue differentiation and lipid deposition. Thus, we observed that *Pparg*-P465L mutation on *Ins2*-Akita background significantly reduced adipose tissue mass and adipocytokine levels as measured by plasma leptin and adiponectin. Reduced plasma adiponectin and leptin could contribute to whole-body insulin resistance. However, liver and skeletal muscle of LA mice were equally insulin sensitive to those of WA mice, indicating that the signaling downstream of these peptides are intact. Possibly the extent of decrease in adiponectin and leptin is not sufficient to alter the insulin sensitivity in liver and muscles. However, the LA mice had adipocytes significantly reduced in number but larger in size, which are shown to be associated with reduced insulin sensitivity (33), suggesting the inability of the adipose tissue to recruit new preadipocytes. The higher plasma triglyceride, and a slight increase in liver triglyceride content, observed in LA females could also be a consequence of this impaired storage function of the adipose tissue. Similar to our observation, Gray et al. reported that leptin-deficient *ob/ob* mice carrying the *Pparg*-P465L mutation had a significant reduction in adipose tissue mass and are insulin resistant (13). The authors attributed this to an inability of the adipose tissue to expand in the face of increased availability of energy. Our in vitro data using adipose tissue explants and primary adipocytes suggest that LA adipose tissues also have impaired insulin-stimulated glucose uptake, further confirming their adipose tissue dysfunction. Whereas our conclusions were derived using Akita mutation as a source of insulin deficiency, rendering *Pparg*-P465L mutant mice insulin deficient by other means such as Streptozotocin treatment and/or treating our model with various antidiabetic drugs may provide further insight into the phenotype.

Although our study was focused on *Ins2*<sup>Akita/+</sup> females, the same mechanisms must be responsible for the increased severity of diabetes in LA males compared with WA males. Diabetes induced by *Ins2*-Akita mutation affects males more severely than females (34), and consequently, only males are used as models of type 1 diabetes in general. However, our study shows that *Pparg*-P465L mutation significantly increases hyperglycemia in Akita female and advocates the use of female *Ins2*<sup>Akita/+</sup> mice as an excellent model to study diabetes, particularly in female-specific conditions including polycystic ovary syndrome and gestational diabetes. Our mice also provide a model where reduced insulin and insulin resistance, signatures of type 1 and type 2 diabetes, respectively, are simultaneously present.

In conclusion, our study showed that *Pparg*-P465L mutation worsens the hyperglycemia caused by diabetogenic *Ins2*-Akita mutation and has unmasked the insulin-resistance phenotype in the adipose tissue of mice carrying the *Pparg*-P465L mutation on *Ins2*-Akita background. A simultaneous reduction of PPAR $\gamma$  and insulin, which are both critical in adipocyte differentiation, leads to limited expansion of adipose tissues in these mice. The primary storage defect in adipose tissue triggers hypertriglyceridemia. Adipose tissue insulin resistance also increases pressure on an already stressed pancreas and contributes to a further destruction of  $\beta$ -cells and reduc-



tion in circulating plasma insulin. This, in turn, causes the liver to upregulate gluconeogenesis, resulting in the enhanced hyperglycemia.

#### ACKNOWLEDGMENTS

This work was supported by funding from National Institutes of Health grants HL-042630, HL-87946, and DK-067320. No potential conflicts of interest relevant to this article were reported.

A.A.P. designed and performed experiments and wrote the manuscript. L.A.J. designed and performed experiments, contributed to discussion, and reviewed/edited the manuscript. Y.-S.T. contributed to discussion and reviewed/edited the manuscript. N.M. contributed to designing experiments and discussion and wrote the manuscript.

The authors thank Dr. Hyung-Suk Kim, University of North Carolina-Chapel Hill (UNC-CH), for help with gene expression analysis, Longquan Xu, UNC-CH, for BP measurements, and Sabrina Baxter, UNC-CH, for technical assistance. The authors are grateful to Drs. Oliver Smithies, Nobuyuki Takahashi, Jose M. Arbones-Mainar, Kumar Pandya, and Feng Li for scientific discussion and thank Benjamin Bleasdale, Raymond Fox, and Dr. Hirofumi Tomita, UNC-CH, for critical reading of the manuscript.

#### REFERENCES

- Koutnikova H, Cock TA, Watanabe M, Houten SM, Champy MF, Dierich A, Auwerx J. Compensation by the muscle limits the metabolic consequences of lipodystrophy in PPAR gamma hypomorphic mice. *Proc Natl Acad Sci U S A* 2003;100:14457–14462
- Berger J, Moller DE. The mechanisms of action of PPARs. *Annu Rev Med* 2002;53:409–435
- Deeb SS, Fajas L, Nemoto M, Pihlajamäki J, Mykkänen L, Kuusisto J, Laakso M, Fujimoto W, Auwerx J. A Pro12Ala substitution in PPAR-gamma2 associated with decreased receptor activity, lower body mass index and improved insulin sensitivity. *Nat Genet* 1998;20:284–287
- Ristow M, Müller-Wieland D, Pfeiffer A, Krone W, Kahn CR. Obesity associated with a mutation in a genetic regulator of adipocyte differentiation. *N Engl J Med* 1998;339:953–959
- Barroso I, Gurnell M, Crowley VE, Agostini M, Schwabe JW, Soos MA, Maslen GL, Williams TD, Lewis H, Schafer AJ, Chatterjee VK, O'Rahilly S. Dominant negative mutations in human PPARgamma associated with severe insulin resistance, diabetes mellitus and hypertension. *Nature* 1999;402:880–883
- Barak Y, Nelson MC, Ong ES, Jones YZ, Ruiz-Lozano P, Chien KR, Koder A, Evans RM. PPAR gamma is required for placental, cardiac, and adipose tissue development. *Mol Cell* 1999;4:585–595
- Kubota N, Terauchi Y, Miki H, Tamemoto H, Yamauchi T, Kameda K, Satoh S, Nakano R, Ishii C, Sugiyama T, Eto K, Tsubamoto Y, Okuno A, Murakami K, Sekihara H, Hasegawa G, Naito M, Toyoshima Y, Tanaka S, Shiota K, Kitamura T, Fujita T, Ezaki O, Aizawa S, Kadowaki T. PPAR gamma mediates high-fat diet-induced adipocyte hypertrophy and insulin resistance. *Mol Cell* 1999;4:597–609
- Rosen ED, Sarraf P, Troy AE, Bradwin G, Moore K, Milstone DS, Spiegelman BM, Mortensen RM. PPAR gamma is required for the differentiation of adipose tissue in vivo and in vitro. *Mol Cell* 1999;4:611–617
- Gavrilova O, Haluzik M, Matsusue K, Cutson JJ, Johnson L, Dietz KR, Nicol CJ, Vinson C, Gonzalez FJ, Reitman ML. Liver peroxisome proliferator-activated receptor gamma contributes to hepatic steatosis, triglyceride clearance, and regulation of body fat mass. *J Biol Chem* 2003;278:34268–34276
- Evener AL, He W, Barak Y, Le J, Bandyopadhyay G, Olson P, Wilkes J, Evans RM, Olefsky J. Muscle-specific Pparg deletion causes insulin resistance. *Nat Med* 2003;9:1491–1497
- Rosen ED, Kulkarni RN, Sarraf P, Ozcan U, Okada T, Hsu CH, Eisenman D, Magnuson MA, Gonzalez FJ, Kahn CR, Spiegelman BM. Targeted elimination of peroxisome proliferator-activated receptor gamma in beta cells leads to abnormalities in islet mass without compromising glucose homeostasis. *Mol Cell Biol* 2003;23:7222–7229
- Tsai YS, Kim HJ, Takahashi N, Kim HS, Hagaman JR, Kim JK, Maeda N. Hypertension and abnormal fat distribution but not insulin resistance in mice with P465L PPARgamma. *J Clin Invest* 2004;114:240–249
- Gray SL, Nora ED, Grosse J, Manieri M, Stoeger T, Medina-Gomez G, Burling K, Wattler S, Russ A, Yeo GS, Chatterjee VK, O'Rahilly S, Voshol PJ, Cinti S, Vidal-Puig A. Leptin deficiency unmasks the deleterious effects of impaired peroxisome proliferator-activated receptor gamma function (P465L PPARgamma) in mice. *Diabetes* 2006;55:2669–2677
- Wang J, Takeuchi T, Tanaka S, Kubo SK, Kayo T, Lu D, Takata K, Koizumi A, Izumi T. A mutation in the insulin 2 gene induces diabetes with severe pancreatic beta-cell dysfunction in the Mody mouse. *J Clin Invest* 1999;103:27–37
- Roehrig KL, Allred JB. Direct enzymatic procedure for the determination of liver glycogen. *Anal Biochem* 1974;58:414–421
- Thalman S, Juge-Aubry CE, Meier CA. Explant cultures of white adipose tissue. *Methods Mol Biol* 2008;456:195–199
- Arbones-Mainar JM, Johnson LA, Altenburg MK, Maeda N. Differential modulation of diet-induced obesity and adipocyte functionality by human apolipoprotein E3 and E4 in mice. *Int J Obes (Lond)* 2008;32:1595–1605
- Farkas MH, Swift LL, Hasty AH, Linton MF, Fazio S. The recycling of apolipoprotein E in primary cultures of mouse hepatocytes. Evidence for a physiologic connection to high density lipoprotein metabolism. *J Biol Chem* 2003;278:9412–9417
- González-Rodríguez A, Nevado C, Escrivá F, Sesti G, Rondinone CM, Benito M, Valverde AM. PTP1B deficiency increases glucose uptake in neonatal hepatocytes: involvement of IRA/GLUT2 complexes. *Am J Physiol Gastrointest Liver Physiol* 2008;295:G338–347
- Suh HN, Lee YJ, Han HJ. Interleukin-6 promotes 2-deoxyglucose uptake through p44/42 MAPKs activation via Ca<sup>2+</sup>/PKC and EGF receptor in primary cultured chicken hepatocytes. *J Cell Physiol* 2009;218:643–652
- Gliemann J, Osterlind K, Vinten J, Gammeltoft S. A procedure for measurement of distribution spaces in isolated fat cells. *Biochim Biophys Acta* 1972;286:1–9
- McGrowder D, Ragoobirsingh D, Brown P. Modulation of glucose uptake in adipose tissue by nitric oxide-generating compounds. *J Biosci* 2006;31:347–354
- Laffel L. Ketone bodies: a review of physiology, pathophysiology and application of monitoring to diabetes. *Diabetes Metab Res Rev* 1999;15:412–426
- Londos C, Honnor RC, Dhillon GS. cAMP-dependent protein kinase and lipolysis in rat adipocytes. III. Multiple modes of insulin regulation of lipolysis and regulation of insulin responses by adenylate cyclase regulators. *J Biol Chem* 1985;260:15139–15145
- Weyer C, Funahashi T, Tanaka S, Hotta K, Matsuzawa Y, Pratley RE, Tataranni PA. Hypoadiponectinemia in obesity and type 2 diabetes: close association with insulin resistance and hyperinsulinemia. *J Clin Endocrinol Metab* 2001;86:1930–1935
- Shimomura I, Hammer RE, Ikemoto S, Brown MS, Goldstein JL. Leptin reverses insulin resistance and diabetes mellitus in mice with congenital lipodystrophy. *Nature* 1999;401:73–76
- Lara-Castro C, Garvey WT. Intracellular lipid accumulation in liver and muscle and the insulin resistance syndrome. *Endocrinol Metab Clin North Am* 2008;37:841–856
- Evans-Molina C, Robbins RD, Kono T, Tersey SA, Vestermark GL, Nunemaker CS, Garney JC, Deering TG, Keller SR, Maier B, Mirmira RG. Peroxisome proliferator-activated receptor gamma activation restores islet function in diabetic mice through reduction of endoplasmic reticulum stress and maintenance of euchromatin structure. *Mol Cell Biol* 2009;29:2053–2067
- Pilkis SJ, Granner DK. Molecular physiology of the regulation of hepatic gluconeogenesis and glycolysis. *Annu Rev Physiol* 1992;54:885–909
- Kim SY, Kim HI, Park SK, Im SS, Li T, Cheon HG, Ahn YH. Liver glucokinase can be activated by peroxisome proliferator-activated receptor-gamma. *Diabetes* 2004;53(Suppl. 1):S66–S70
- Iynedjian PB, Gjinovci A, Renold AE. Stimulation by insulin of glucokinase gene transcription in liver of diabetic rats. *J Biol Chem* 1988;263:740–744
- Magnuson MA, Andreone TL, Printz RL, Koch S, Granner DK. Rat glucokinase gene: structure and regulation by insulin. *Proc Natl Acad Sci U S A* 1989;86:4838–4842
- Salans LB, Knittle JL, Hirsch J. The role of adipose cell size and adipose tissue insulin sensitivity in the carbohydrate intolerance of human obesity. *J Clin Invest* 1968;47:153–165
- Yoshioka M, Kayo T, Ikeda T, Koizumi A. A novel locus, Mody4, distal to D7Mit189 on chromosome 7 determines early-onset NIDDM in nonobese C57BL/6 (Akita) mutant mice. *Diabetes* 1997;46:887–894